Acta Cryst. (1986). B42, 121-130

High-Resolution Electron-Microscopic Study of the Modulated Structure of Kostovite ($Cu_{1-x}Au_{1+x}Te_4$)

BY G. VAN TENDELOO AND S. AMELINCKX*

Rijksuniversitair Centrum Antwerpen (RUCA), Groenenborgerlaan 171, 2020-*Antwerpen, Belgium*

(*Received* 20 *May* 1985; *accepted* 2 *September* 1985)

Abstract

The modulated structure of kostovite ($AuCuTe_4$) is shown to be closely related to that of sylvanite ($AuAgTe_4$). Well ordered stoichiometric kostovite has a commensurate superstructure of the idealized calaverite structure ($AuTe_2$). A long-period antiphase-boundary modulated structure, which produces an apparently incommensurate diffraction pattern, is found in the non-stoichiometric samples. A detailed model is presented for this structure. Chemically disordered specimens exhibit a displacement-modulated structure related to that of calaverite. It is suggested that in the ternary compounds, displacements as well as antiphase-boundary modulations occur, the two modes being interrelated, whereas in calaverite only displacement modulations are present. These conclusions are based on the results of a study by means of electron diffraction and high-resolution electron microscopy and on *in situ* heating experiments.

1. Introduction

In previous papers we have studied the synthetic compounds $AuTe_2$, $AuAgTe_4$ and $Au_{0.75}Ag_{0.25}Te_2$ which are also known under their respective mineralogical names calaverite, sylvanite and krennerite (Van Tendeloo, Gregoriades & Amelinckx, 1983*a*, *b*, 1984). It was demonstrated by means of electron diffraction and high-resolution electron microscopy that $AuTe_2$ has an incommensurate modulated structure. Near-stoichiometric sylvanite has a commensurate ordered superstructure derived from that of $AuTe_2$, whereas off-stoichiometric sylvanite has an incommensurate modulated structure derived from that of $AuTe_2$, but based also on the periodic arrangement of antiphase-boundary-like interfaces. Finally krennerite has a commensurate twin interface modulated superstructure derived from that of calaverite. These observations were found to be in agreement with the structures, determined by means of X-ray diffraction by Tunell & Pauling (1952). However, the latter authors have neglected weak reflections and thus overlooked the modulated character of the structure of calaverite, which was first noted by Sueno, Kimata & Ohmasa (1979).

It was suggested by Terziev (1966) that the Cu-substituted analogues of sylvanite and krennerite might be isomorphous with their Ag counterparts. It is the purpose of this paper to demonstrate that this is largely, but not entirely, the case and moreover to show also that these compounds have either commensurate or incommensurate modulated structures depending on composition and on heat treatment. The modulation turns out to be closely similar in nature to that of the Ag homologues.

2. Materials and specimen preparation

The materials were prepared by melting together the constituent elements in evacuated quartz tubes at 823 K followed by slow cooling over several days. We prepared materials with compositions close to $Au_{0.5}Cu_{0.5}Te_2$ and $Au_{3/4}Cu_{1/4}Te_2$ which we expected to be the Cu homologues of, respectively, sylvanite and krennerite.

Specimens for electron microscopy are prepared by crushing fragments of the ingots and depositing the small flakes on a Cu grid dipped in glue.

3. Crystal structures

The Cu homologue of sylvanite, as far as its composition is concerned, known also as the mineral kostovite, is also assumed to be isostructural with sylvanite (Terziev, 1966) from the similarity of the powder diffraction patterns. The sylvanite structure, as determined by Tunell & Pauling (1952), is represented in Fig. 1(*b*), viewed along the *b* axis and along the *a* axis; the substitution of Ag by Cu would lead to the proposed kostovite structure. In sylvanite the Ag atoms are alternatively shifted up and down along the *b* axis, as is evident from the *a* view, doubling in this way the size of the unit cell as compared to that

* Also at SCK/CEN, B 2400-Mol, Belgium. Work performed under the auspices of the Association RUCA-SCK and with financial support from IIKW, Brussels.

0108-7681/86/020121-10$01.50

of calaverite (Fig. 1*a*); in the latter compound all heavy metal positions are occupied by Au.

The projection of the actual positions of the Te atoms (small full dots in Fig. 1) differs somewhat from the ideal ones (small open dots), leading to a deformation of the Te octahedra around the heavy atoms.

Since we have not yet found evidence for the Cu homologue of the krennerite phase we shall not describe the structure of this phase.

4. Diffraction patterns

4.1. *Commensurate phase*

The $[010]_{cal}$ diffraction patterns of commensurate sylvanite ($AuAgTe_2$) and commensurate kostovite ($AuCuTe_2$) are compared in Fig. 2(*a*) and (*b*). A calaverite-type diffraction pattern is shown for comparison in Fig. 3(*a*) or in Fig. 5 in the paper by Van Tendeloo *et al.* (1983*a*). The sylvanite and kostovite patterns are indexed on the sylvanite unit cell, whereas the calaverite pattern is indexed on the unit cell of the idealized structure of calaverite as proposed by Tunell & Pauling (1952). It is quite clear that the ordering of Ag and Au causes the projected unit cell of sylvanite to be double in size as compared to that of calaverite. The 00*l* (l = odd) reflections such as 001 in sylvanite are most often absent along the [010] zone; when present they are very weak as in Fig. 2(*a*). These reflections are present in other zones, however.

This is related to the fact that in sylvanite the displacements of the Ag atoms from their ideal positions, with respect to the Au sublattice, are predominantly along the [010] direction.

In kostovite weak reflections of this type, in particular 001, are more often observed at the centres of the pseudo-rectangles in the [010] zones; they are indicated by arrows in Fig. 2(*b*); such spots cannot be produced by double diffraction. Their presence presumably means that in kostovite the displacements have a small component parallel with the *b* plane. We shall see below that the high-resolution images possibly suggest this. It is not excluded that this also occurs to some extent in sylvanite but that in this case the difference in atomic scattering amplitude between Ag and Au was too small to produce any visible spot, whereas it is larger in kostovite.

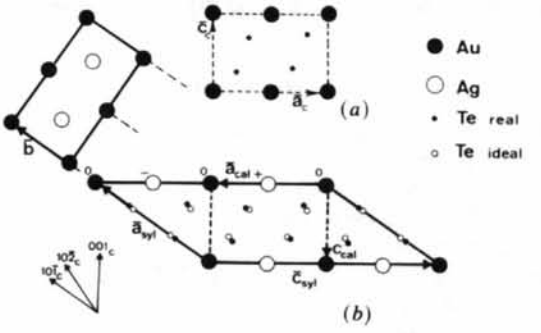

Fig. 1. Crystal structure of calaverite and sylvanite. (*a*) Calaverite: the large circles represent heavy metal atoms; the small circles are Te. (*b*) Sylvanite: the unit cell is two times larger than that of calaverite. Three viewing directions are indicated with respect to the calaverite structure by means of arrows.

4.2. *Incommensurate phase*

4.2.1. *The* [010] *zone.* Diffraction patterns of two different types, both incommensurate, were observed in a specimen with composition in the vicinity of $Au_{0.75}Cu_{0.25}Te_2$. The first type of pattern (Fig. 3*a*) is quite similar to that observed in calaverite and in non-stoichiometric sylvanite. The basic spots can be indexed on a unit cell with lattice parameters $a \approx 0{\cdot}72$, $b = 0{\cdot}44$, $c = 0{\cdot}51$ nm, which are practically the same as those of calaverite.

Sequences of satellites, in the same configuration as in calaverite, are associated with each basic spot, *i.e.* one only observes even orders, namely the second- and fourth-order satellites. One possible wavevector, **q** (Fig. 4), is $1{\cdot}089\ nm^{-1}$ and encloses an angle of 6·5° with the [202]* direction (Fig. 3*a*). The diffraction pattern is thus incommensurate; in Fig. 3(*a*) it is indexed on a calaverite-like lattice.

In a second type of diffraction pattern (Fig. 3*b*) the same **q** vector can be chosen; it is not significantly different from that of the first type of pattern. The geometry of the spot pattern is thus similar but now

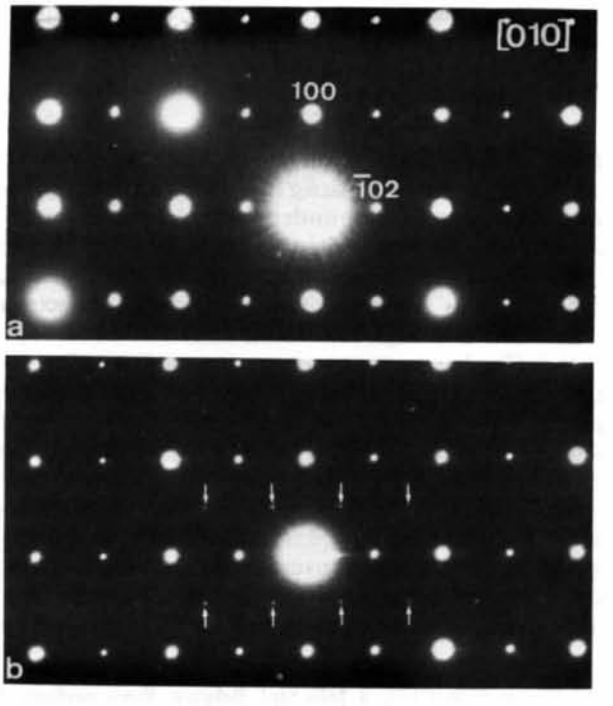

Fig. 2. Electron diffraction patterns along the [010] zone: (*a*) sylvanite; (*b*) kostovite.

the odd orders, *i.e.* the first- and third-order satellites, are prominently visible next to the even orders. The satellite configuration in this pattern is represented schematically in Fig. 4 and compared with that actually observed. The spots numbered (1), (2), (3), (4) belong to I and the spots (1′), (2′), (3′), (4′) to II. Interpretations in terms of wavevectors other than **q** are also possible as we shall see below.

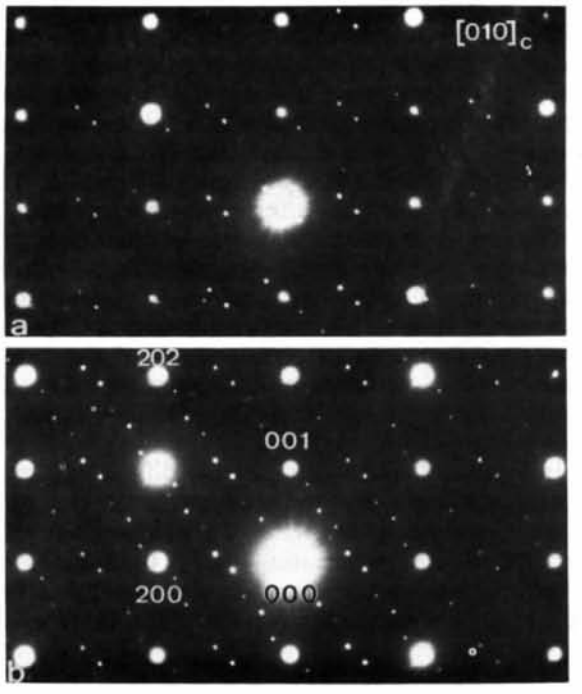

Fig. 3. 'Incommensurate' electron diffraction patterns along the [010] zone of kostovite. (*a*) Only even-order satellites are present. (*b*) Satellites of all order are present.

4.2.2. *The* $[10\bar{2}]$ *zone.* The $[10\bar{2}]_{cal}$-zone diffraction pattern is reproduced in Fig. 5; the spots in the rows with k = odd are split; sequences of satellite spots have suffered a fractional shift over $\frac{1}{2}$ with respect to the basic spots. Along the rows of spots k = even the satellite sequences are not shifted with respect to the basic spots, which are thus unsplit. These satellites could possibly be due to a double diffraction. The segments connecting the satellites are slightly inclined with respect to the normal to the $[010]_{cal}$ direction. If it is assumed that the spot sequences are due to periodic antiphase boundaries the direction of these boundaries must be roughly perpendicular to the $[201]_{cal}$ direction. The fractional shifts are consistent with a $\frac{1}{2}[110]_{cal}$ displacement vector. One has $\mathbf{R} \cdot \mathbf{g} = \frac{1}{2}[110] \cdot [hkl]^* = \frac{1}{2}(h+k)$; since in the zone considered only spots with h = even are present, the dot product is $\frac{1}{2}k$, *i.e.* $\frac{1}{2}$(mod 1) for k = odd and 0(mod 1) for k = even.

4.3. *Temperature dependence*

When a kostovite specimen producing a commensurate diffraction pattern is heated in the heating holder of the microscope the weak spots indicated by arrows in Fig. 2(*b*) disappear first. This specimen is further transformed into a specimen producing an 'incommensurate' pattern containing satellites of all orders. This transformation is irreversible; Fig. 6 shows the diffraction patterns of the same area of the same specimen before and after heating; both photographs were taken at room temperature.

Further heating of such a specimen, or a specimen initially producing an incommensurate diffraction pattern, does not lead to appreciable changes in the magnitude or in the direction of the **q** vector, but it

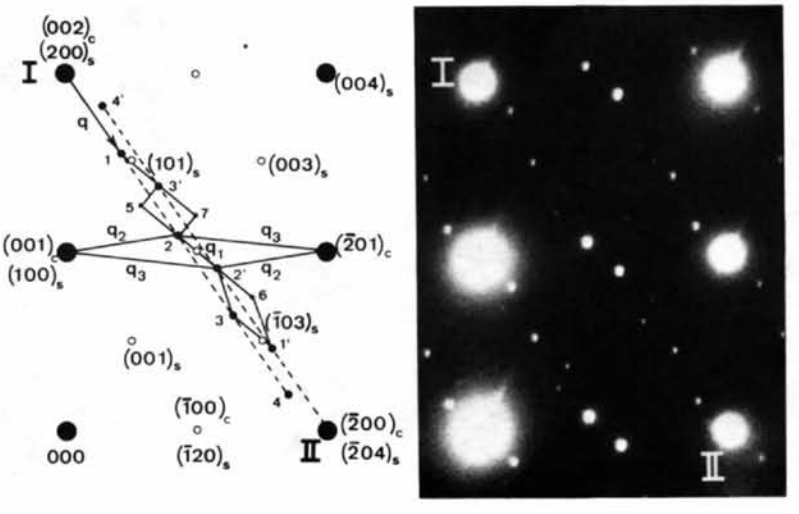

Fig. 4. Schematic representation of the satellites belonging to the spots I and II of the diffraction pattern of Fig. 3(*b*). Different possible **q** vectors are indicated.

does change the intensity of the satellites. In the [010]-zone pattern the odd-order satellites disappear first; it is only close to the melting temperature that the even-order satellites also disappear. This phenomenon is again not reversible. When a specimen which has been brought into the temperature range where the odd-order satellites vanish is cooled again to room temperature in the microscope holder (*i.e.* fairly rapidly) only the even-order satellites remain. The fourth-order satellite is very weak or invisible, even though the second-order satellite is intense. This suggests that the fourth-order satellite is not due to double diffraction; this possibility could not be excluded in the case of sylvanite (Van Tendeloo *et al.*, 1983*b*).

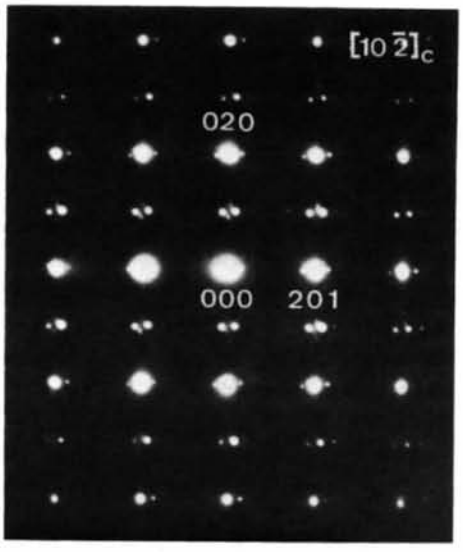

Fig. 5. Diffraction pattern of incommensurate kostovite along the $[10\bar{2}]_{cal}$ zone. Note the fraction shifts $\frac{1}{2}$ along the rows of split spots with k = odd. The direction of the splitting encloses a small angle with the normal to [010].

These experiments seem to indicate that the presence of satellites reflects a form of order which disappears in two or three stages with increasing temperature. The non-reversibility is consistent with our assumption that atomic order, among Cu and Au, is involved, which could only be restored by sufficiently slow cooling or by annealing at lower temperatures.

The persistence of the second-order satellites is also consistent with our model whereby the even-order satellites in the [010] zone are related to small displacements in the Te sublattice and (or) to displacements parallel with the (010) plane of the heavy atoms. Only close to the melting point would the Te lattice become 'ideal', *i.e.* as described by Tunell & Pauling (1952) for calaverite.

In some specimens of calaverite diffuse and relatively weak spots are observed between the two most intense satellite spots, *i.e.* at the $h0l$ position with h = odd. After a small heating pulse in the microscope these diffuse spots disappear irreversibly. They apparently correspond to a metastable situation.

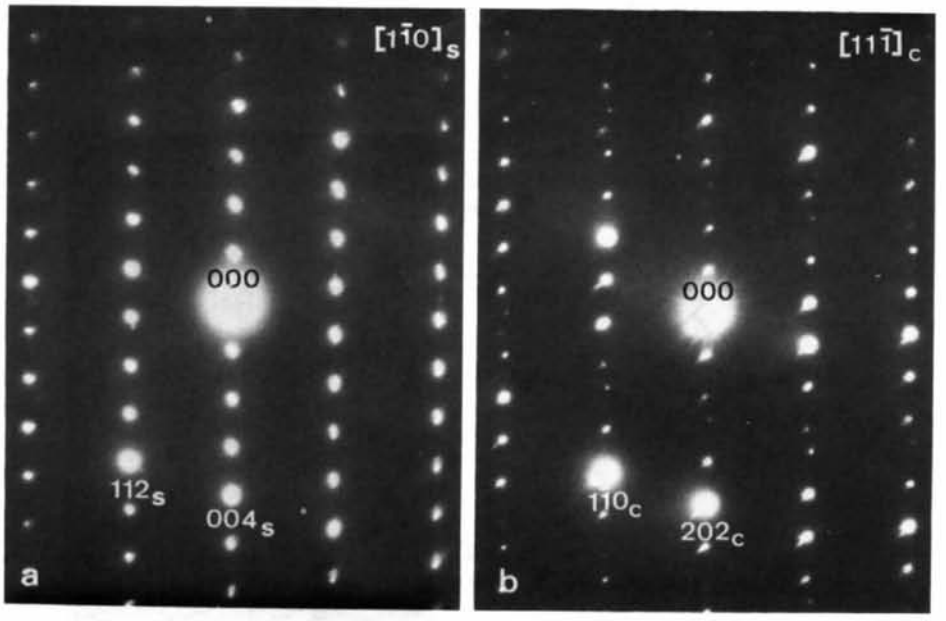

Fig. 6. (*a*) Diffraction pattern of commensurate kostovite along the $[1\bar{1}0]_s$ zone before heating. (*b*) Diffraction patterns from the same area after heating the specimen, followed by cooling. Note that (*a*) is indexed with respect to the sylvanite lattice, whereas (*b*) is indexed with respect to the calaverite lattice.

5. High-resolution images

5.1. *Image calculations*

Although no explicit reference is made in this section to computed images, the interpretation is of course largely based on the images calculated for sylvanite and calaverite in our previous papers and reproduced there (Van Tendeloo *et al.*, 1983*a*, *b*). It was shown that under suitable imaging conditions the bright-dot patterns reflect the geometry of the heavy-atom positions. In thin foils, and along certain zones also the Te arrangement can be visualized as bright dots. The images of kostovite are not appreciably different from those of sylvanite under the same diffraction conditions.

5.2. *The commensurate phase*

5.2.1. *The* [010] *zone.* We have pointed out above that the diffraction pattern along the [010] zone exhibits weak reflections of the type $00l$ (with l = odd). The image corresponding to this diffraction pattern is reproduced in Fig. 7. The brightest dots have the geometry of the heavy-atom columns. When viewed at grazing incidence along the $[201]_s \equiv [001]_c$ rows it becomes evident that alternating rows have a slightly different intensity consistent with the assumption that alternating rows contain respectively Au and Cu columns. On the other hand, when viewed along the $[001]_s \equiv [100]_c$ rows it becomes clear that all the rows of bright dots are now on the average equally bright but they are not quite straight; they form a zigzag sequence. These small displacements parallel with the (010) plane are presumably responsible for the appearance of the weak reflections indicated by arrows in Fig. 2.

5.2.2. *The* $[100]_{syl}$ *direction.* The small displacements along the [010] direction can in principle be revealed in an image along the $[10\bar{1}]_{cal}$ direction ($[100]_s$ zone) along which the two types of heavy atoms occur in separate columns, which also contain Te atoms, however. This is shown in Fig. 8, where the inset represents the diffraction pattern. The difference in brightness is therefore not very pronounced. On viewing the photograph under grazing incidence the [010] rows parallel with the straight arrow appear straight whereas the [001] rows parallel with the broken arrow appear slightly zigzag shaped, in accordance with the structure as represented in Fig. 1.

5.2.3. *The* $[001]_{cal} \equiv [201]_{syl}$ *zone.* An image along this zone, which is pseudo-hexagonal, is represented in Fig. 9 where the inset (*c*) shows the corresponding diffraction pattern. Along this zone we have a 'column' structure and all atom columns are in fact revealed in the image. The projected structure at the same magnification as Fig. 9(*b*) is shown schematically in the lower inset. The configuration of dots is consistent with the interpretation whereby the most intense bright dots represent heavy atoms. In the thickest parts of the specimen these brightest dots have two different intensities, corresponding to Au and Cu (or Ag in sylvanite) atom columns. Each of these bright dots is surrounded by a hexagon of dots with a weaker brightness corresponding to Te columns, consistent with the projection of the structure. In the thinnest part of the specimen there are no significant differences in dot brightness. The slight relative displacements in the [010] direction of heavy atoms cannot be revealed in this section since a given column contains atoms which have suffered upward displacements as well as downward ones; the average position which is the same along all columns is thus revealed.

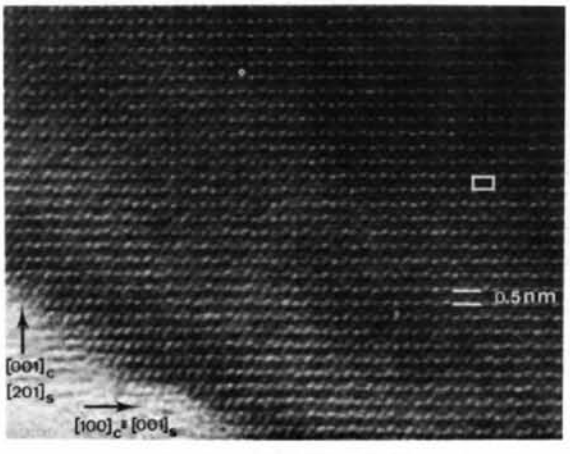

Fig. 7. High-resolution image of commensurate kostovite along the [010] zone. The $[100]_c$ rows are zigzag shaped.

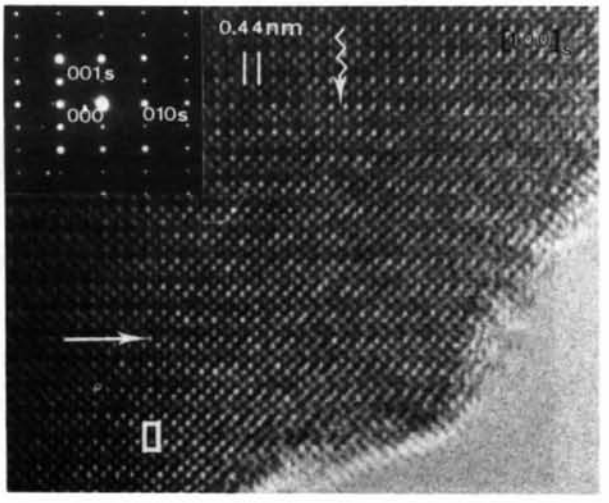

Fig. 8. High-resolution image along the $[100]_{syl}$ direction. The inset shows the corresponding diffraction pattern. The [010] rows are straight (straight arrow) whereas the (001) rows are zigzag shaped (broken arrow).

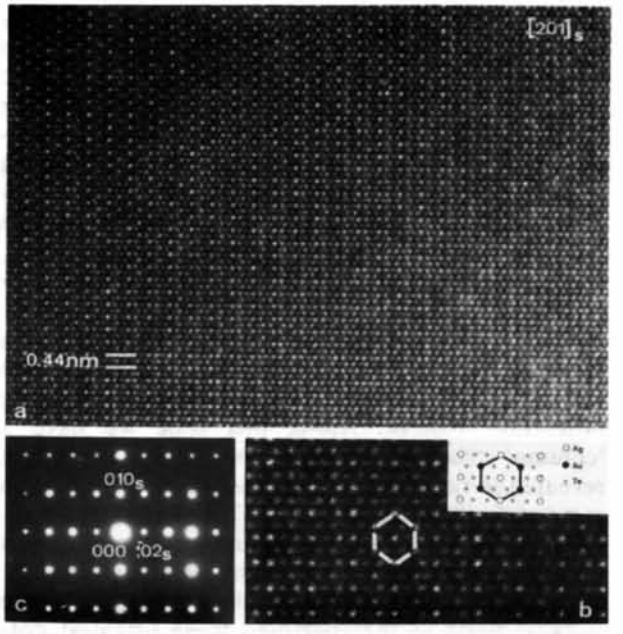

Fig. 9. (*a*) High-resolution image along the pseudo hexagonal $[001]_{cal} \equiv [201]_{syl}$ zone. (*b*) Magnified part of (*a*) revealing clearly all atom columns; the inset shows the projected structure along the same zone and at the same magnification for sylvanite; in kostovite Ag is replaced by Cu. (*c*) The corresponding diffraction pattern.

5.3. *The incommensurate phase*

5.3.1. *The* [010] *zone image.* High-resolution images were obtained along different zones. Particularly significant images are obtained along the [010] zone. The image of Fig. 10 originates from a region producing a diffraction pattern of the second type, *i.e.* like Fig. 3(*b*).

Comparison with the representation of the sylvanite structure of Fig. 1 shows that all atom columns are apparently visualized in the region of the image which corresponds to the thinnest part of the specimen. The projected calaverite-type unit cell is indicated in Fig. 10(*a*).

Intensity modulations along the $[001]_c$ atom rows are quite obvious especially when the photograph of Fig. 10(*c*) is viewed under grazing incidence along the indicated lines, or along the arrow (1) in Fig. 10(*d*). Linear sequences of four or five brighter dots alternate with sequences of darker dots along the [001] rows. The loci of darkest dots give rise to a system of rather closely spaced dark fringes along direction (2) enclosing an angle of ~4° with the [001] rows. A similar system of fringes is formed along direction (3) which encloses an angle of ~3° with the same dot rows (Fig. 10*d*).

Along the [010] viewing direction the two kinds of heavy atoms, Au and Cu, occupy alternatively $[001]_c$

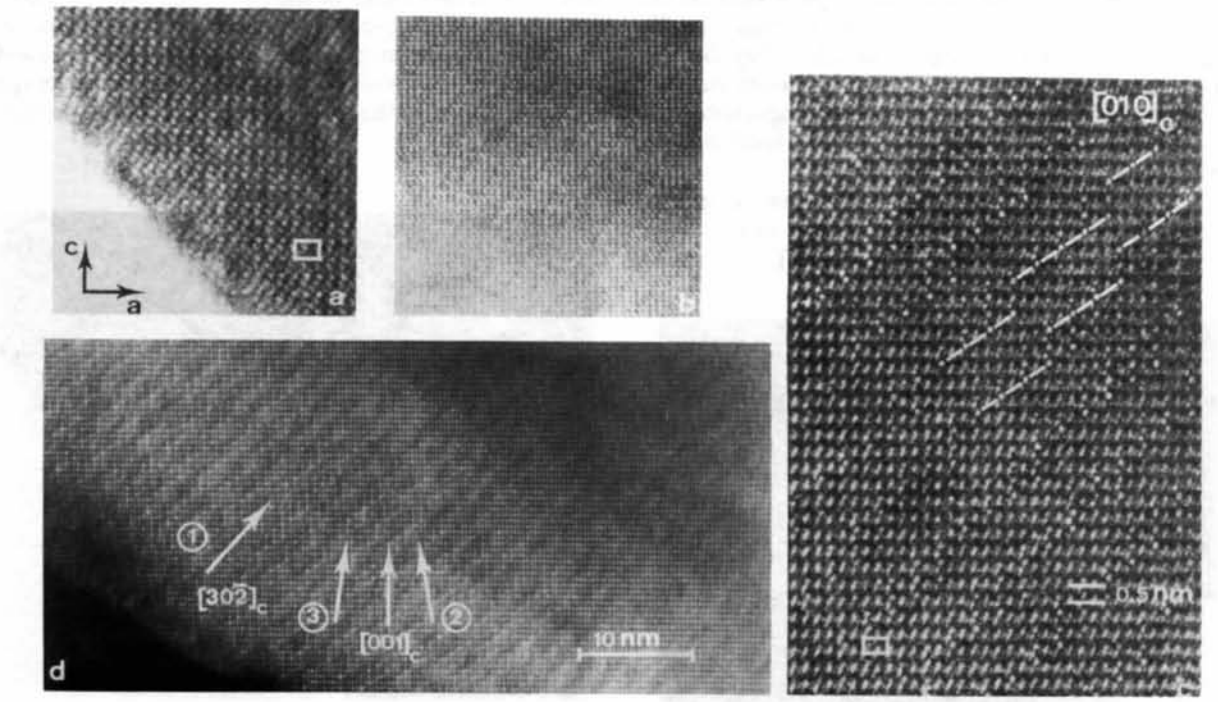

Fig. 10. High-resolution image along the [010] zone of 'incommensurate' kostovite. (*a*) Thinnest part of the specimen; all atom columns are revealed. (*c*) Magnified part of (*b*) exhibiting extra bright dots along the antiphase boundaries. (*d*) Low-magnification, dark-field, high-resolution image revealing the antiphase boundaries in a thicker part of the specimen. When viewed at grazing incidence along the $[001]_c$ rows brightness modulations are quite obvious. Fringes are visible along the indicated directions (1), (2) and (3).

rows of columns in commensurate sylvanite (Fig. 1). It is suggested that since kostovite is assumed to be isostructural with sylvanite, the difference in brightness of the dots in the present case is presumably related to the occupation of alternating atom rows by Au and Cu.

As in sylvanite the intensity modulation along the $[001]_{cal}$ rows can thus be explained by assuming that periodic antiphase-boundary-like interfaces are present along the (302) planes, as represented schematically in Fig. 11(*a*). Along the antiphase boundaries a row of Au atoms continues as a row of Cu atoms and *vice versa*, the Te sublattice remaining continuous across the interfaces.

The intensity modulations giving rise to the fringes of type (2) (Fig. 10) are described by a wavevector $\mathbf{q}_2$ (Fig. 11), whereas the fringes of type (3) (Fig. 10) are similarly described by a wavevector $\mathbf{q}_3$(Fig. 11). The periodic arrangement of antiphase boundaries gives rise to a modulation with wavevector $\mathbf{q}_1$.

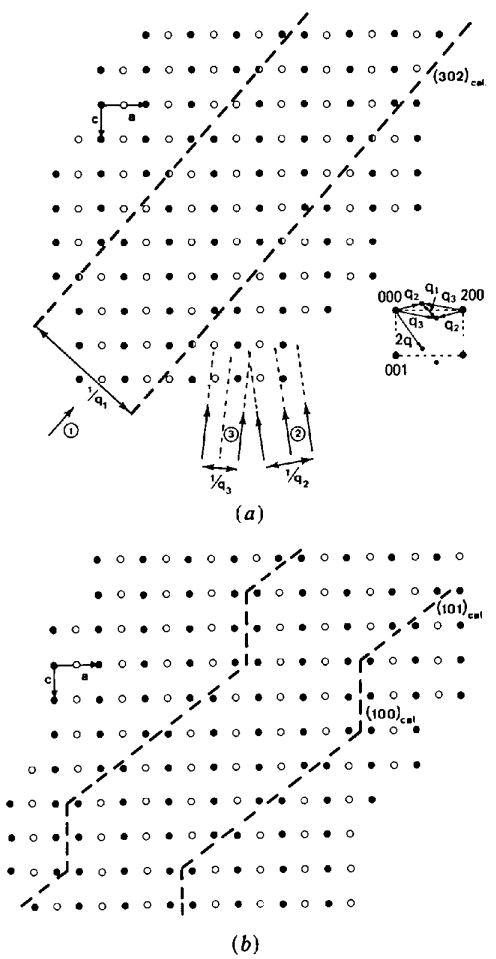

Fig. 11. (*a*) Idealized model for periodic antiphase boundaries in kostovite along the $(302)_{cal}$ planes. Only heavy metal atoms are shown. Along the $[001]_c$ direction the atom rows are occupied in part by Cu and in part by Au; the occupation changes along the antiphase boundaries. The $\mathbf{q}$ vectors corresponding to different modulation waves are shown as well. (*b*) Realistic model where the periodic antiphase boundaries are in part along the $(100)_{cal}$ and $(101)_{cal}$ planes.

If the Te lattice is assumed to be ideal and continuous across these boundaries, the interfaces are truly antiphase boundaries with a displacement vector $\frac{1}{2}[110]_{cal}$ or $\frac{1}{4}[021]_{syl}$. This displacement vector connects a Cu and a Au position, and in the ideal Te sublattice it is a lattice vector. In the real Te sublattice the Te atoms occupy slightly displaced positions in calaverite as well as in sylvanite and strictly speaking the interfaces are not antiphase boundaries. Moreover, a modulation of the Te sublattice accompanies the modulation due to the antiphasing. The structure is thus simultaneously interface and deformation modulated; with the same $\mathbf{q}$ vector since both modulations are intimately coupled.

We shall see that the diffraction pattern as well as the high-resolution images can consistently be interpreted on such a model.

On the other hand, the images of Figs. 10(*b*) and 10(*c*), taken along the same [010] zone, exhibit more clearly the traces of the interfaces as lines of somewhat brighter dots. It now becomes evident that the antiphase boundaries have in fact a zigzag shape as presented in Fig. 11(*b*). They are piece-wise situated in $(101)_{cal}$ planes, which thus seem to be a low-energy interface, and contain notches or ledges along $(100)_{cal}$ planes. Their average orientation thus becomes parallel with the trace of the $(302)_{cal}$ plane.

5.3.2. *The* $[10\bar{2}]$ *image.* When viewed along the $[10\bar{2}]$ zone the image of Fig. 12 is obtained. It is quite obvious that the brightness of the spots along lines normal to [010] is modulated with a period of about 12–13 interspot distances. The brightness profile of alternating spot rows is 'in phase' whereas in successive rows it is in 'antiphase', *i.e.* the brightest part in one spot row corresponds to the darkest part in the following row. The switching over occurs fairly gradually along lines roughly parallel with the [010] direction; these lines are traces of planes which are roughly parallel with the [010] direction; their direction is not strictly defined.

According to the model, discussed below, these planes are in fact the same antiphase boundaries which are also observed in the [010] zone.

The average direction of these antiphase boundaries is perpendicular to the segment connecting the spot pairs in the corresponding diffraction pattern of Fig. 5, obtained along the same zone; it is clear that this segment is not quite perpendicular to [010] as noted above.

5.4. *Model*

A somewhat idealized commensurate model based on these observations is represented in Fig. 13. The projected unit cell is outlined in heavy lines. The

relationship between the base vectors of the superstructure cell and that of calaverite is:

$$\begin{bmatrix}\mathbf{A}_1\\ \mathbf{A}_3\end{bmatrix}=\begin{bmatrix}4 & -6\\ -\frac{5}{2} & -2\end{bmatrix}\begin{bmatrix}\mathbf{a}\\ \mathbf{c}\end{bmatrix}_{\text{cal}}.$$

The pattern almost repeats with a quasi unit cell defined by the base vectors $\frac{1}{2}\mathbf{A}_1$ and $\mathbf{A}_3$. The difference between the two halves of the unit cell involves a different occupation of three atom positions. The large unit cell will thus lead to quasi extinctions in the diffraction pattern.

6. Optical diffraction

In order to verify the rather complex model of the 'incommensurate' phase we have performed an optical diffraction experiment using a demagnified negative of the dot pattern (without any lines of course) represented in Fig. 13 as an optical grating. This model represents the structure as viewed along the [010] zone. Two sizes of dots were used to represent the Au and Cu heavy atoms. As the largest scatterer is Au, it is modelled by the larger dots. It is quite obvious that along the antiphase boundaries rows of large dots continue as rows of small dots and *vice versa*. The Te columns which, in this section, have the basic periodicity have not been included since they would mainly intensify the basic reflections, but not give rise to satellites. The optical diffraction pattern is represented in Fig. 14; it is quite obvious that it correctly represents the electron diffraction pattern of the incommensurate phase along the [010] zone shown in Fig. 3.

As the other satellites are related to displacements along the (010) plane, they do not show up since such displacements were not included in the model, which only simulates the effect of the antiphasing of the heavy-atom rows.

7. Discussion

The diffraction patterns could be interpreted in terms of deformation modulation as well as in terms of an interface modulated structure.

The sequence of spots (1), (2), (3), (4) in Fig. 4 can for instance be considered as being the satellites of successive orders produced by the wavevector **q** starting from I, *i.e.* $(002)_c$ or $(200)_s$. However, a prominent intensity modulation corresponding to this

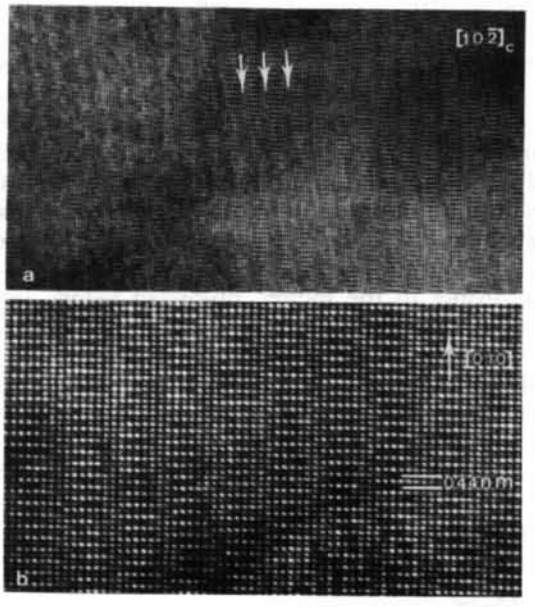

Fig. 12. High-resolution image of the [10$\bar{2}$] zone of incommensurate kostovite. The directions of the antiphase boundaries are indicated in the low-magnification image (*a*). A magnified view is shown in (*b*).

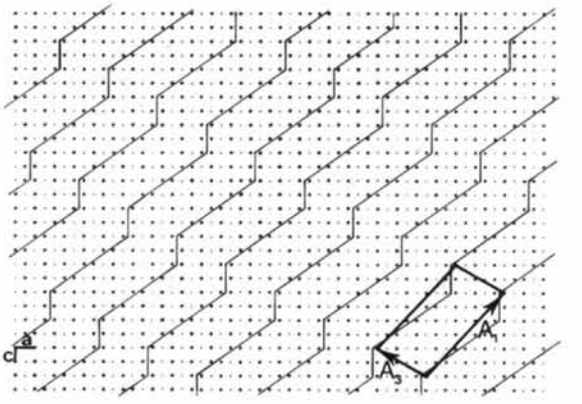

Fig. 13. Model of the 'incommensurate' kostovite structure. Only the projections of the heavy metal atoms are represented as dots of two different sizes. The unit cell of the superstructure resulting from the periodic antiphase boundaries is outlined.

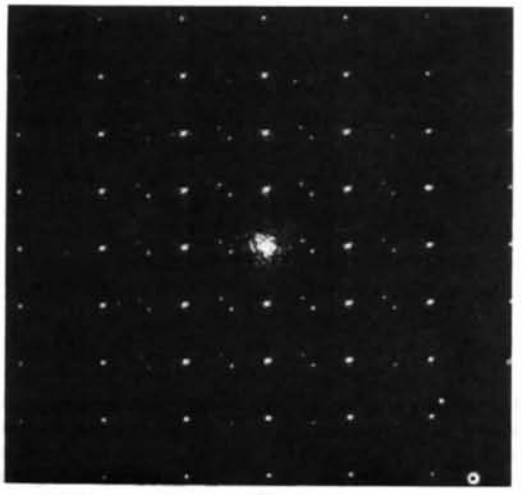

Fig. 14. Optical diffraction pattern obtained from an optical grating made from a demagnified negative of the dot pattern in Fig. 13, omitting the lines.

wavevector **q** is not discernible in the image of Fig. 10. A similar **q** vector also occurs in calaverite and in incommensurate sylvanite and it was attributed to a displacement modulation wave affecting the Te sublattice, since in this material only the even orders are weakly visible in the [010] zone.

It was shown by Van Tendeloo *et al.* (1983*a*, *b*) that the pairs of spots (2) (2′) could also be attributed to the splitting of the $(002)_{syl}$ spot as a result of the presence of periodic antiphase-boundary-like interfaces with a spacing $1/\mathbf{q}_1$ and a displacement vector $\frac{1}{2}[110]_c \equiv \frac{1}{4}[021]_s$.

In the present investigation we also found intense spots of odd order (1) and (3) as well as (1′) and (3′). If our model is to be consistent with the diffraction patterns also these spots should be related to the occurrence of periodic antiphase boundaries. The spot pairs (1) and (3′) and (3) and (1′), which are connected with vectors which are equivalent with the vector connecting the spot pairs (2) (2′), should in particular also be consistent with this model. The spot pair (1) and (3′) can be considered as resulting from the splitting of the spot $(101)_s$; the fractional shift deduced from the displacement vector $\frac{1}{4}[021]_s$ is then for this spot $\frac{1}{4}[021] \cdot [101] = \frac{1}{4} (\text{mod } 1)$ which is consistent with the observed fractional shift.

Similarly, the spot pair (3) and (1′) is derived by splitting from the spot $(\bar{1}03)_s$; the calculated fractional shift is $\frac{3}{4} (\text{mod } 1)$, again in agreement with the observations. It should be noted that the fractional shifts of the satellite sequences are consistent with the proposed displacement vector for *all* reflections.

The weak spots of types (5) and (6) have also occasionally been observed in the Cu homologues; they are the second-order reflections in the sequence of satellites (5), (2), (2′), (6) due to the periodic antiphase boundaries and associated with the $(\bar{1}01)_c$ spot. They are presumably more visible in the present compound than in sylvanite because the atomic scattering amplitudes of Cu and Au differ more than do those of Ag and Au, giving rise to more intense superstructure reflections. Also, other spot pairs such as (1) and (3′) or (3) and (1′) sometimes give rise to weak second-order satellites.

The high-resolution image along the [010] zone reproduced in Fig. 10 is also consistent with the proposed models of Figs. 11 and 13.

The sets of lines (1), (2) and (3) (Fig. 10), which represent the traces of planes perpendicular to the drawing in Fig. 11, provide in fact alternative descriptions of the structure. The set (1) (Fig. 11*a*) separates domains which both contain rows of the two kinds of heavy atoms, but in an antiphase relationship.

On the other hand, the sets (2) and (3) separate domain strips which contain only one type of heavy atom in successive strips; the heavy-atom rows are alternating, however. It turns out that the sets of interfaces with traces along (2) and (3) give rise to well defined fringes which can be observed by viewing under grazing incidence along the indicated arrows (2) and (3) in Fig. 10. The spacings in these two sets of fringes are not the same, in agreement with the model.

The interfaces with traces along (1), on the other hand, give rise to broader and much less well defined fringes.

As already mentioned by Van Tendeloo *et al.* (1983*a*) the modulated structure of calaverite is presumably quite similar to that of sylvanite in the sense that in calaverite all heavy metal atoms are of course Au. This similarity is suggested by the close resemblance of the geometry of the satellite configurations in the two compounds, the intensity of the satellites in calaverite being much smaller in the [010] zone.

The structure of calaverite could thus be modulated by the relative displacement of the Au atoms belonging to one sublattice with respect to those of the other sublattice; as represented schematically in an exaggerated fashion in Fig. 15. Such a structure may give rise to antiphase-boundary-like interfaces with a displacement vector $\frac{1}{2}[110]_{cal}$ (Fig. 15*a*).

Since such displacements are all along the [010] direction no satellite would be visible in the [010]-zone pattern. However, the displacements of the Au atoms are accompanied by small displacements of the Te atoms also, the latter displacements having a component perpendicular to the [010] direction, and

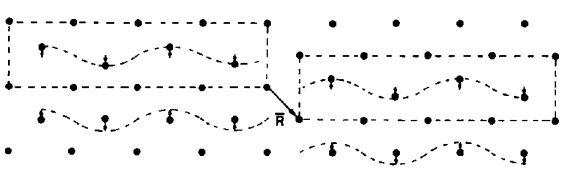

(*a*)

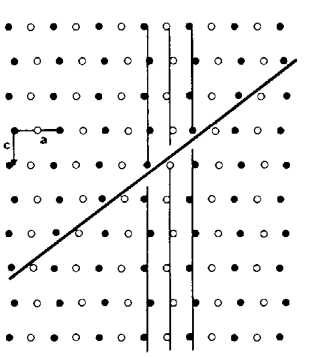

(*b*)

Fig. 15. Possible models for the antiphasing in calaverite ($AuTe_2$). (*a*) Displacement modulation along [010]. (*b*) Displacement modulation parallel with (010).

thus giving rise to even-order satellites visible in the [010] zone.

The observations of Fig. 7 suggest that the displacements of the heavy atoms may also have a small component along the [010] plane; this is represented schematically in Fig. 15(*b*) which is a projection of the Au atoms on the *b* plane of calaverite. Along the periodic interfaces the phase of the displacement pattern may change gradually along the heavy lines. Such interfaces could be described as discommensuration walls. A set of periodic discommensuration walls situated in the same planes as the antiphase boundaries in the model of Fig. 11 would produce a diffraction pattern which is similar in geometry to that of Fig. 3. The coupling of the displacement wave with the ordering between Cu and Au could for instance occur in the same way as suggested for sylvanite (Van Tendeloo *et al.*, 1983*b*).

The behaviour of the diffraction pattern as a function of temperature supports our assumption that the modulated structure is due to the coupling of deformation modulation and atomic antiphasing. The deformation or displacement modulation with wave vector $2\mathbf{q}$ is reversible and is very similar in all three compounds, calaverite, sylvanite and kostovite. On the other hand, the ordering of Ag and Au (in sylvanite) and of Cu and Au (in kostovite) is not reversible; annealing and slow cooling is required to reestablish the atomic order. This produces a modulated structure with wavevector $\mathbf{q}$. The way in which coupling may be understood is described by Van Tendeloo *et al.* (1983*b*).

Whereas in calaverite the modulation wave described by the wavevector $\mathbf{q}_1$ is planar [see, for example, Fig. 7 of Van Tendeloo *et al.* (1983*a*)] this is no longer the case in kostovite. The coupling with the composition wave so as to form antiphase boundaries apparently causes the interfaces, described by $\mathbf{q}_1$, to become ledged (Fig. 11*b*), thereby keeping the same average orientation, however. The antiphase boundaries apparently have a strong preference for the simple crystallographic planes (101) and (100). Moreover, the difference in atomic scattering amplitude between Au and Cu causes the satellites to have a larger intensity in kostovite than in the other compounds.

8. Concluding remarks

All high-resolution images as well as all diffraction patterns in kostovite and sylvanite can consistently be explained either in terms of the ordered structure of commensurate kostovite (*i.e.* the sylvanite structure) or of a long-period 'incommensurate' antiphase-boundary derivative of this, modelled in Fig. 11.

However, the type of atomic order that exists in the ternaries sylvanite and kostovite, and which is assumed to be responsible for the periodic antiphase boundaries, *cannot* occur in the binary compound calaverite. Nevertheless the diffraction pattern of calaverite is almost identical, except for some extinctions and some differences in intensity, with that of the incommensurate ternaries. Over and above the atomic order commensurate sylvanite was shown to exhibit also position modulation mainly of the heavy atoms but also of the Te atoms as shown in Fig. 1. Since a calaverite-type diffraction pattern remains after a heat treatment that disturbs the chemical ordering it is reasonable to assume that in calaverite the position modulation remains. Whereas the ternaries exhibit both chemical ordering and position modulation, with the same period, it is only position modulation that occurs in calaverite.

Langouche (1985) has performed Mössbauer spectrometry of the ^{125}Te and ^{129}Te isotopes in kostovite and calaverite and found appreciable broadening of the absorption peaks, which is consistent with the occurrence of different environments of these nuclei in a displacement-modulated structure.

We would like to thank Dr Langouche for drawing our attention to the analogy between kostovite and sylvanite.

References

LANGOUCHE, G. (1985). Private communication.

SUENO, S., KIMATA, M. & OHMASA, M. (1979). *AIP Conf. Proc.* pp. 333-335.

TERZIEV, G. (1966). *Am. Mineral.* **51**, 29-39.

TUNELL, G. & PAULING, L. (1952). *Acta Cryst.* **5**, 375-381.

VAN TENDELOO, G., GREGORIADES, P. & AMELINCKX, S. (1983*a*). *J. Solid State Chem.* **50**, 321-334.

VAN TENDELOO, G., GREGORIADES, P. & AMELINCKX, S. (1983*b*). *J. Solid State Chem.* **50**, 335-361.

VAN TENDELOO, G., GREGORIADES, P. & AMELINCKX, S. (1984). *J. Solid. State Chem.* **53**, 281-289.